# Thermal— mechanical strain characterization for printed wiring boards

by T. Y. Wu Y. Guo W. T. Chen

Multilayer printed wiring boards are widely used in electronic packaging assemblies. One critical reliability concern is the thermal-mechanical strains induced by temperature change. For example, the in-plane strain affects the thermal fatique life of surface mount solder interconnections, while the outof-plane strain affects the mechanical integrity of the plated-through holes of the printed wiring boards. For this paper, a systematic study of the thermal-mechanical strain of epoxy-glass printed wiring boards, below and above the glass transition temperatures of the epoxies, has been carried out. The study includes measurements of properties of basic constituent materials (epoxy, glass fabric, copper), of intermediate building blocks in the fabrication process, and of final products. The study has led to a quantitative engineering model that predicts the average in-plane thermal-mechanical strain for use in modeling surface mount components on a printed wiring board, as well as the average out-of-plane

thermal-mechanical strain for determining plated-through-hole reliability in thermal shock processes. The model was verified by two experimental techniques (measurement by thermomechanical analyzer, and moiré interferometry) applied to two epoxy resins and three glass fabrics, with and without copper planes. For thermal shock below the glass transition temperatures of the epoxy resins, the in-plane and out-of-plane strains are described by a modified rule-of-mixtures theory and a biaxial plane stress model, respectively. For temperatures above the glass transition temperatures, the in-plane strains are governed by the copper and glass fabric. whereas the out-of-plane strains are dominated by the incompressible fluid behavior of the epoxy resins. The nonuniform pattern of thermal expansion in regions populated with plated-through holes was examined. The reliability of surface mount solder interconnections and plated-through holes is discussed.

**Copyright** 1993 by International Business Machines Corporation. Copying in printed form for private use is permitted without payment of royalty provided that (1) each reproduction is done without alteration and (2) the *Journal* reference and IBM copyright notice are included on the first page. The title and abstract, but no other portions, of this paper may be copied or distributed royalty free without further permission by computer-based and other information-service systems. Permission to *republish* any other portion of this paper must be obtained from the Editor.

# Introduction

Thermally induced strain often dictates the mechanical reliability of electronic packages associated with multilayer printed wiring boards (PWBs). Potential reliability problems include failures in solder interconnections between the PWB and surface mount components and failures in the PWB itself. Failures in the solder interconnections (see the other papers in this issue on Solder Ball Connect technology) are primarily due to shear deformation, which is related to the mismatch of in-plane (x-y) plane in Figure 1) thermal displacements between the PWB and the surface mount components. Failures in the PWB itself, including cracks in plated-through holes (PTHs) and copper foil, cracks in epoxy resin, and delamination between epoxy-to-glass and epoxy-to-copper interfaces, are primarily due to tensile deformation, which is related to the mismatch of out-of-plane (z-direction in Figure 1) thermal displacements between various constituents of the PWB. The importance of the in-plane and out-of-plane strains depends on the overall design, assembly, and temperature range. For example, the out-ofplane strain is of particular concern in thick PWBs when temperature exceeds the glass transition temperatures of the epoxy resin,  $T_g^{er}$ . Sophisticated modeling tools, such as the finite element method, can be utilized to predict stress and strain distribution in PWBs [1-3]. To obtain accurate predictions, the coefficients of thermal expansion (CTEs) of all component materials as well as the average thermal-mechanical deformation characteristics of the PWBs are needed as inputs to the models.

PWBs are designed and manufactured with a variety of glass fabric types, resins, glass-to-resin ratios, and copper plane thicknesses to meet the performance and cost requirements of the user application [4]. Figure 1 is a schematic of a typical manufacturing process flow for a glass-fabric-reinforced PWB. The process begins with the impregnation of woven-glass fabric with an epoxy resin to form an epoxy-glass laminate-in essence, a layer of glass fabric between two layers of epoxy resin. Several such epoxy-glass laminates are then sandwiched between copper foil layers and laminated at elevated temperature and pressure into an epoxy-glass-copper core. Circuits are then printed on the core by means of photolithographic processes, and the core is subjected to hole-drilling and copper-plating processes, if necessary. The multilayer PWB is fabricated by stacking several cores, separated with additional epoxy-glass laminates and copper foils, and repeating the lamination, hole-drilling, photolithographic (on the top surface) and copper-plating processes [4].

New resins and reinforcement fabrics are being developed to provide specific performance and engineering cycle-time improvements over the widely used FR-4 epoxy and E-glass PWBs [5–7]. To achieve cost and engineering

cycle-time reduction, it is imperative to have the ability to predict, in the early design stages, both the in-plane and out-of-plane thermal strains for the PWB, below as well as above  $T_g^{er}$ . This information is essential both for assessing compatibility between the PWB and surface mount component designs (e.g., leadframe and solder-pad designs and solder-joint thicknesses) and for predicting the solder and plated-through-hole reliability of the PWBs. Extensive work has been done in characterizing CTEs for various materials and composites in the in-plane direction [8]. Little is known, however, regarding the out-of-plane expansion, especially at temperatures above  $T_e^{er}$ .

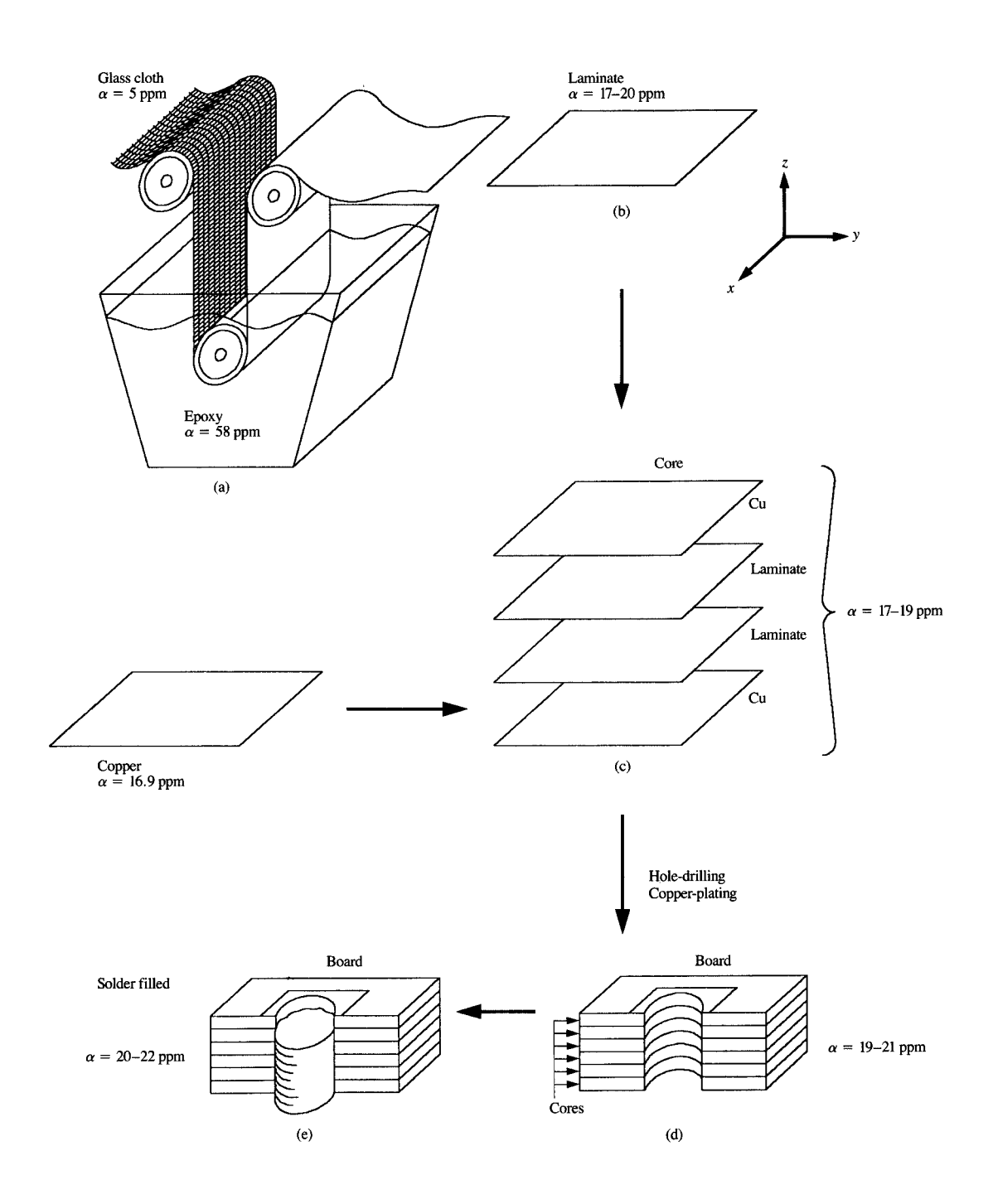
The focus of this paper is to present a simple engineering model, accompanied by systematic experimental measurements and verifications. A threedimensional thermal-mechanical model that can predict the average in-plane and out-of-plane strains for multilayer PWBs, below and above  $T_g^{er}$ , is presented. The model assumes that all individual layers of a PWB composite behave like isotropic elastic thin plates when temperatures are below  $T_{\rm g}^{\it er}$ . When temperatures are above  $T_{\rm g}^{\it er}$ , the epoxy behaves like an incompressible fluid. The effective in-plane and out-of-plane strains for various epoxy-glass laminates, below and above  $T_g^{er}$ , were both numerically predicted by the model and measured by a thermomechanical analyzer. Comparisons between predicted and experimental results are presented. The effects of the proportions of epoxy, glass, and copper in the laminates are closely examined. A moiré interferometry technique, more accurate than the thermomechanical analyzer, was adopted to examine the variations of inplane strain of a PWB over a larger area. The experimental procedures of the moiré interferometry are briefly discussed. Results showing the strain distribution in areas with and without plated-through holes are presented. Finally, the implications of the current work for system reliability are discussed-specifically, how in-plane strain affects the fatigue performance of solder joints and how out-of-plane strain affects the plated-through-hole integrity.

# Thermal-mechanical strain characterization

In this section, a simple engineering model is presented. Epoxy-glass laminates, with and without added copper foil layers, were chosen as an example. The methodology is extendable to a wider range of multilayer composites, as long as the assumptions (stated in the following sections) are satisfied.

For simplicity, the thermal-mechanical strains of the epoxy-glass laminate are expressed in terms of effective coefficients of thermal expansion (CTEs), defined as the average thermal-mechanical strains per unit change in temperature (ppm/°C or 10<sup>-6</sup>/°C). The in-plane effective

 $<sup>\</sup>overline{1}$  In this paper, "laminate" may refer to a simple epoxy-glass-epoxy structure or to such a structure with an additional copper plane.



# Floure

Schematic showing a typical process flow for a multilayer printed wiring board, including (a) epoxy impregnation, (b) epoxy–glass laminate, (c) epoxy–glass–copper core, (d) multilayer composite with plated-through holes, and (e) multilayer composite with solder-filled plated-through holes.

CTEs, below and above  $T_{\rm g}^{er}$ , are denoted by  $\alpha_{\rm x}$  and  $\hat{\alpha}_{\rm x}$ , respectively, while the out-of-plane effective CTEs are denoted by  $\alpha_{\rm z}$  and  $\hat{\alpha}_{\rm z}$ , respectively. The caret refers to temperatures above  $T_{\rm e}^{er}$ .

• In-plane effective CTE for temperatures below  $T_g^{er}$  For a composite with n isotropic thin layers, let  $E_i$ ,  $\nu_i$ , and  $\alpha_i$  respectively denote Young's modulus, Poisson's ratio, and the CTE for the ith layer of material (i=1,n). If the edge effects are ignored, the effective in-plane Young's modulus for the composite,  $E_{x-y}^{eff}$ , and the effective in-plane CTE,  $\alpha_{x-y}^{eff}$ , can be expressed as functions of  $E_i$ ,  $\alpha_i$ , and volume fractions,  $V_i$  (volume occupied by the ith layer divided by the total volume of the composite), as

$$E_{xy}^{eff} = \sum_{i=1}^{n} E_i V_i \tag{1}$$

and

$$\alpha_{xy}^{eff} = \frac{\sum_{i=1}^{n} \alpha_{i} E_{i} V_{i}}{E_{xy}^{eff}}.$$
 (2)

Equations (1) and (2) are the so-called "rule-of-mixtures" and "modulus-modified rule-of-mixtures." These elementary relations are commonly used for engineering estimates of elastic composites [8]. Note that Poisson's ratios  $\nu_i$  do not appear in these equations. Hill [9] and Schapery [10] have shown that for a two-component (n = 2) unidirectional-fiber composite system, the approximations of Equations (1) and (2) deviate from exact solutions by terms that are proportional to  $(\nu_1 - \nu_2)^2$  and  $\nu_1 - \nu_2$ , respectively. While the effect of Poisson's ratio on the accuracy of Equation (1) is typically very small, the effect on Equation (2) is not always negligible. For example, Schapery [10] has shown that when

$$(\alpha_1, E_1, \nu_1) = (60 \text{ ppm/°C}, 3 \text{ GPa}, 0.382)$$

and

$$(\alpha_2, E_2, \nu_2) = (4.9 \text{ ppm/°C}, 67.6 \text{ GPa}, 0.2),$$

the maximum deviation of Equation (1) from the exact solution is less than 3.4%, whereas the maximum deviation of Equation (2) can be as much as 30%.

When applying Equations (1) and (2) to calculate the inplane effective CTE of an epoxy-glass laminate (with or without copper foil), we make the following idealizations. First, woven-glass-fabric layers, epoxy-resin layers, and copper foil layers are all treated as individual isotropic thin plates. Rigorously speaking, woven-glass fabric is at best orthotropic. However, moiré interferometry measurements (discussed in a later section) on cross-ply (90° rotation between adjacent layers) epoxy-glass laminates indicate very little CTE anisotropy between the x and y directions, with no observable shear distortion. This implies that transverse (in-plane) isotropy is a reasonable assumption, at least with regard to the CTE. The selection of out-of-plane modulus and CTE for the glass, on the other hand, has little impact on the accuracy of the out-of-plane CTE prediction, since the out-of-plane expansion is dominated by the epoxy. Therefore, without loss of generality, woven-glass fabric can be treated as isotropic with regard to the CTE.

The second idealization is neglecting the effects of different Poisson's ratios. That is, all materials—hence the composite—are assumed to have the same Poisson's ratio  $(\nu_i = \nu^{eff} = \nu$ , for all i). As previously mentioned, this is a good approximation when Poisson's ratios are close (e.g., Poisson's ratios of both copper and epoxy resin are approximately 0.3); however, when Poisson's ratios are very different (e.g., Poisson's ratio of glass is approximately 0.18), the effect can be significant. Here, it is assumed that the effect of different Poisson's ratios can be accounted for by a set of penalty functions, described as follows.

The third idealization is that a set of penalty functions can be assigned to compensate for the deviations of epoxy-glass laminates and their internal interfaces from the elastic idealizations of Equations (1) and (2) and the previous two idealizations. Such deviations include the effect of different Poisson's ratios, variance from bulk properties due to small size and irregular geometry, loss of interfacial adhesion, formation of voids, localized inelastic deformation, etc. These factors depend upon material combinations, local geometry (e.g., type of glass fabric), coupling agents (adhesion promoters), surface treatments, and process conditions. They are, in general, very difficult if not impossible to quantify. In the present work, a phenomenological approach is adopted. The collective influences of these factors are quantified by means of a set of engineering parameters (penalty functions) whose values are directly determined by experiments.

Equations (1) and (2) are modified to include the penalty functions:

$$E_{xy}^{eff} = \sum_{i=1}^{n} P_i E_i V_i \tag{3}$$

and

$$\alpha_{xy}^{eff} = \frac{\sum_{i=1}^{n} G_{i} \alpha_{i} E_{i} V_{i}}{E_{x}^{eff}} . \tag{4}$$

A pair of penalty functions,  $P_i$  and  $G_i$ , is needed for each material. They depend not only on the material in the ith layer, but also on the materials in the neighboring i-1 and i+1 layers, to account for any interfacial characteristics associated with the ith layer. For example, the core depicted in Figure 1 is an eight-layer composite consisting of copper-epoxy-glass-epoxy-epoxy-glassepoxy-copper. Three pairs of penalty functions are needed to describe this core: one for the copper layers, which depends on the copper and interactions between copper and epoxy; one for the glass, which depends on the glass fabric and interactions between glass and epoxy; and one for the epoxy, which depends on the epoxy itself, interactions between epoxy and copper, and interactions between epoxy and glass fabric. For most PWBs, these three sets of penalty functions are sufficient to describe the in-plane CTE. If more materials are included, the number of penalty functions increases accordingly.

These penalty functions can be determined by a series of experiments. For example, to determine the penalty functions for a given glass fabric (interfacing with a given epoxy), first measure Young's modulus and the in-plane CTE of the glass fabric and of the epoxy; then, fabricate a laminate using the glass fabric and epoxy, and measure the effective Young's modulus and the effective in-plane CTE of the laminate; finally, determine the penalty functions by simultaneously fitting Equations (3) and (4) to the measured modulus and CTE values. The same process can be repeated to include other proportions of epoxy and glass, material sets, and configurations. The numerical fitting process is somewhat arbitrary, since the number of equations is less than the number of unknowns [e.g., for a two-component system, there are two equations, (3) and (4), versus four unknowns  $(P_1, G_1, P_2, G_2)$ ]. The penalty functions may not be unique; however, they should be chosen so that the same set of functions can provide "best-fit" correspondence to all of the measured data. The penalty functions can be as simple as a set of constants or as complex as a set of functionals that depend on local parameters, such as material combination, local geometry, dimension, and interfacial characteristics. For a given material set corresponding to a given process, the same penalty functions should be used. The penalty functions are independent of global parameters, such as volume fraction, stacking sequence, total PWB thickness, and structural symmetry. In the special case in which there are no deviations from bulk properties, no defects, and no localized inelastic deformations, the penalty functions would be simply 1, and Equations (3) and (4) would reduce to Equations (1) and (2). In the special case in which the effective in-plane Young's modulus and CTE of the composite show the same dependence on Young's moduli and the volume fractions of the constituents,  $P_i = G_i$  for all i.

- In-plane effective CTE for temperatures above  $T_{\rm g}^{\rm er}$ The in-plane effective CTE for temperatures above  $T_{\alpha}^{er}$  ( $\hat{\alpha}_{\kappa}^{eff}$ ) can also be obtained by Equations (3) and (4), except that the proper "modulus" and CTE corresponding to high temperatures must be used for all layers. For example, above  $T_{g}^{er}$ , Young's modulus for epoxy is not defined, since epoxy is no longer a solid. However, epoxy still maintains a finite resistance to deformation. Tensile test results show that the "modulus" (defined as the initial slope of the stress-strain curve) of epoxy above  $T_g^{er}$  is very low (approximately 0.07 GPa) and continues to decrease as temperature increases. Therefore, the inplane CTE of the laminate is dominated by Young's moduli and the CTEs of the glass-fabric and copper layers, which are nearly unchanged at high temperatures (e.g., at 260°C).
- Out-of-plane effective CTE for temperatures below  $T_{\varrho}^{er}$ The out-of-plane expansion of a composite includes contributions from epoxy, glass fabric, and copper. It consists of free thermal expansion as well as mechanical dilatation due to in-plane stresses associated with in-plane mechanical constraints from the glass fabric and copper. The magnitudes of the in-plane stresses are proportional to differences in CTE values between the epoxy and the epoxy-glass (copper) laminate in the in-plane direction. In the following, a biaxial plane stress model is used to estimate the in-plane stress in the epoxy. Once the stress value is determined, the out-of-plane strain for the epoxy and the laminate are readily determined, as described below. Let  $E^{er}$  and  $\alpha^{er}$  denote Young's modulus and the CTE of the epoxy resin, respectively. The thermal-mechanical strain components in the epoxy resin of an epoxy-glass laminate produced by a temperature increase  $\Delta T$  can be written as

$$\epsilon_{xx} = \alpha^{er} \Delta T + \frac{\sigma_{xx}}{E^{er}} - \frac{\nu}{E^{er}} (\sigma_{yy} + \sigma_{zz}),$$

$$\epsilon_{yy} = \alpha^{er} \Delta T + \frac{\sigma_{yy}}{E^{er}} - \frac{\nu}{E^{er}} (\sigma_{xx} + \sigma_{zz}),$$

$$\epsilon_{zz} = \alpha^{er} \Delta T + \frac{\sigma_{zz}}{E^{er}} - \frac{\nu}{E^{er}} (\sigma_{xx} + \sigma_{yy}),$$

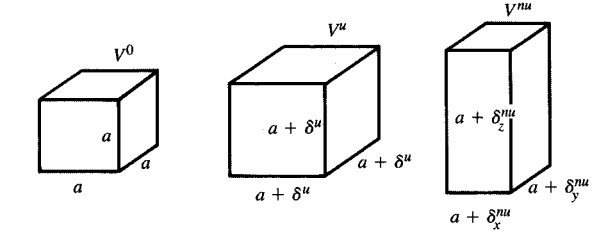
$$\epsilon_{xy} = \epsilon_{yz} = \epsilon_{zx} = 0,$$
(5)

where  $\epsilon$  and  $\sigma$  respectively denote the strain and stress tensor components, and  $\nu$  is the same Poisson's ratio described above in the section *In-plane effective CTE for temperatures below*  $T_g^{er}$ . Since the in-plane strain components of Equation (5) must be equal to  $\alpha_{x\cdot y}^{eff} \Delta T$  as given in Equation (4),

$$\epsilon_{xx} = \epsilon_{yy} = \alpha_{xy}^{eff} \, \Delta T. \tag{6}$$

Assuming a uniform biaxial compressive plane stress  $-\sigma$ , we can write

625



### Flauro

Incompressible element as it undergoes uniform and nonuniform thermal expansion.

$$\sigma_{xx} = \sigma_{yy} = -\sigma, \quad \sigma_{zz} = 0.$$
 (7)

From (5)–(7), we have

$$(\alpha^{er} - \alpha_{x\cdot y}^{eff}) \Delta T = \frac{\sigma}{E^{er}} (1 - \nu), \qquad (8)$$

and the biaxial compressive stress  $\sigma$  in the epoxy resin can be estimated as

$$\sigma = \frac{(\alpha^{er} - \alpha_{xy}^{eff}) \Delta T E^{er}}{(1 - \nu)}.$$
 (9)

Combining Equations (5)–(9), we can derive the effective CTE of the epoxy in the out-of-plane direction, including thermal and mechanical strains, as

$$\alpha_z^{er} = \frac{\epsilon_{zz}}{\Delta T} = \alpha^{er} + \frac{2\nu \left(\alpha^{er} - \alpha_{x,y}^{eff}\right)}{(1 - \nu)}.$$
 (10)

In a typical PWB, the out-of-plane expansion also includes contributions from the glass and copper. The overall effective CTE in the out-of-plane direction can be approximated by

$$\alpha_{\star}^{eff} = V^{Cu} \alpha_{\star}^{Cu} + V^{er} \alpha_{\star}^{er} + V^{glass} \alpha_{\star}^{glass}, \tag{11}$$

where V and  $\alpha$  respectively denote the volume fractions and CTEs for the corresponding materials.

• Out-of-plane effective CTE for temperatures above  $T_g^{er}$ . When the temperature is above  $T_g^{er}$ , the epoxy expands at a greater rate  $(\hat{\alpha}^{er} > \alpha^{er})$ . If there is no external constraint, the expansion is uniform in all directions. For epoxy-glass-copper composites, the in-plane expansion has been observed to be much less than the out-of-plane expansion because of the presence of glass fabric and copper foil, which have relatively lower CTEs and higher Young's moduli, even at high temperatures. If the epoxy

is modeled as an incompressible fluid above  $T_{\rm g}^{\rm er}$ , the total volume change should be identical regardless of whether the expansion is uniform or nonuniform.

Let  $V^0$  denote the initial volume of a cubic epoxy element, as shown in **Figure 2**. If  $V^u$  and  $V^{nu}$  denote the respective volumes of the same element after a uniform and a nonuniform thermal expansion corresponding to a temperature increase of  $\Delta T$ , and  $\delta^u$  and  $\delta^{nu}$  denote the respective changes in linear dimensions,

$$V^{0} = a^{3},$$

$$V^{u} \approx a^{3} + 3\delta^{u}a^{2},$$

$$V^{nu} \approx a^{3} + (\delta^{nu}_{x} + \delta^{nu}_{y} + \delta^{nu}_{z})a^{2}.$$
(12)

Assuming that the element is incompressible  $(V^u = V^{nu})$  and that the in-plane expansion is known  $(\delta_x^{nu} = \delta_y^{nu} = \hat{\alpha}_{xy}^{eff} a \Delta T)$ , we can derive the following relationships:

(7) 
$$3\delta^{u} \approx 2\hat{\alpha}_{xy}^{eff} a\Delta T + \delta_{z}^{nu}$$
,  $\delta_{z}^{nu} \approx 3\hat{\alpha}^{er} a\Delta T - 2\hat{\alpha}_{xy}^{eff} a\Delta T$ ,

(8)  $\hat{\alpha}_{z}^{er} = \frac{\delta_{z}^{nu}}{a\Delta T} \approx (3\hat{\alpha}^{er} - 2\hat{\alpha}_{xy}^{eff})$ . (13)

Thus, the overall out-of-plane effective CTE of an epoxy-glass laminate at temperatures above  $T_{\rm g}^{\rm er}$  can be approximated by Equation (9), using  $\hat{\alpha}_{\rm z}^{\rm er}$  from Equation (13) in place of  $\alpha_{\rm z}^{\rm er}$ , and appropriate values for the copper and glass fabric.

In summary, the in-plane and out-of-plane thermal—mechanical strains, below and above  $T_{\rm g}^{er}$ , can be described completely by Equations (3)–(13).

The validity of the model is subject to a number of restrictions. For example, whether materials can indeed be treated as isotropic elastic thin plates, whether the collective effect of Poisson's ratios and interfacial properties can be described by a single set of penalty functions, whether the plane stress is a good approximation to the state of stress in the laminate, and whether materials truly behave like incompressible fluids when above the glass transition temperature or melting point. It will be shown that these assumptions are indeed good approximations; therefore, the model gives good predictions in the case of woven-glass-reinforced laminates.

# **Experimental and numerical studies**

A systematic plan was defined to quantify the thermal deformation characteristics of PWBs. Samples were fabricated to represent each step of the multilayer PWB fabrication processes, as depicted in Figure 1, including epoxy-glass laminates, epoxy-glass-copper cores, multilayer boards, boards with plated-through holes, and boards with solder-filled plated-through holes. Two epoxies

Table 1 Basic material properties used in calculations.

Material	Poisson's ratio v	Specific gravity ρ	Below $T_{\rm g}^{er}$		Above $T_{\rm g}^{er}$	
			Young's modulus E (GPa)	CTE \alpha (ppm/°C)	Modulus Ê (GPa)	CTE â (ppm/°C)
Copper	0.35	8.96	117	17	117	17
E-glass	0.35	2.54	72.4	5.3	72.4	5.3
FR-4	0.35	1.35	2.4	58	0.07	180
$High-T_g$	0.35	1.55	2.4	52	0.07	175

in combination with three types of glass fabrics were used in the current study. The first epoxy, a Ciba-Geigy FR-4 resin ( $T_{\rm g}^{er}\approx 125^{\circ}{\rm C}$ ), consists of a mixture of brominated diglycidyl ether of bis-phenol A and an epoxidized cresol novolac with dicyandiamide as the hardener. The second epoxy, a Ciba-Geigy resin ( $T_{\rm g}^{er}\approx 175^{\circ}{\rm C}$ ) with higher  $T_{\rm g}^{er}$  (called "high- $T_{\rm g}$ " in the remainder of the paper), consists of an epoxidized cresol novolac and tetrabromobisphenol A hardener with 2 methyl imidazole catalyst. The three glass fabrics are E-glass types 106 (24.7 g/m²), 1080 (49.2 g/m²), and 1675 (96.3 g/m²), each with varying yarn type and weight but the same surface treatment. In all cases, cross-plying and structural symmetry were practiced in preparing the laminates.

The effective CTE of each sample was measured by a Perkin-Elmer Series 7 thermomechanical analyzer (TMA). The temperature range, 20–260°C, covers temperatures below and above the  $T_g^{er}$  of both epoxies. At least three measurements were performed for each sample in the in-plane and out-of-plane directions. Resin weight percentages were determined by burning off the epoxy and measuring the weight of the glass that remained. Young's moduli of glass fabric and copper foil were measured by tensile test, at 20°C and 260°C, using an MTS-810 hydraulic machine with an environmental chamber. The moduli of the epoxies were measured at five different temperatures: 20°C, 50°C, 100°C, and the  $T_g^{er} \pm 10$ °C (i.e., 115°C and 135°C for the FR-4; 165°C and 185°C for the high- $T_a$  resin). Three tests were performed at each temperature; TMA and tensile test results indicated that the modulus and CTE values for the glass and copper remained almost unchanged between 20°C and 260°C. For the epoxies, the modulus and CTE values showed less than 10% variation between 20°C and 100°C; when temperatures were within  $\pm 10^{\circ}$ C of  $T_{g}^{er}$ , a decrease of the modulus values and an increase of the CTE values were observed: beyond the transition region, the CTE values remained nearly constant, while the modulus value dropped to 0.07 GPa.

In the numerical calculation, for the sake of simplicity, we made the following idealizations for the material properties of the epoxies. First, the transition of CTE near

 $T_{\rm g}^{\rm er}$  was ignored (i.e., CTE was assumed to have one constant value before  $T_g^{er}$  and another constant value after  $T_{\rm g}^{\it er}$ ). Second, the modulus was also assumed to have a constant value before  $T_g^{er}$  and another constant value after  $T_{\sigma}^{er}$ . Finally, the small variation of specific gravity with respect to temperature change was ignored. These idealizations were made, since they greatly reduced the complexity of the calculation without affecting the accuracy of the overall CTE predictions. The effect of the transition region of the CTE on the overall thermal strain can easily be assessed, using the current scheme [Equations (12) and (13)], by a lower-bound analysis (assuming that  $T_g^{er}$  is 10°C above the actual  $T_g^{er}$ ) and an upper-bound analysis (assuming that  $T_g^{er}$  is 10°C below the actual  $T_{g}^{er}$ ). The selection of modulus values for the epoxies at temperatures above  $T_g^{er}$  has little impact on CTE predictions, since in-plane thermal strain (above  $T_{\alpha}^{er}$ ) is dominated by the copper and glass, whereas out-of-plane thermal strain does not depend on the modulus. Material properties used in the calculations are listed in Table 1.

In determining the penalty functions for the in-plane CTE prediction, we assumed, for simplicity,  $P_i = G_i$  for all materials. That is, the effective CTE and modulus were assumed to have the same dependence on Young's moduli and volume fractions of the individual constituents. This simplification enabled us to determine the penalty function P for each material by simply fitting Equation (4) to the measured CTE data, rather than simultaneously fitting Equations (3) and (4) to determine P and G. It will be shown that reasonable in-plane CTE predictions were obtained, even with this simplified assumption (if P and G are treated separately, predictions can be further improved). On the basis of this assumption, it turned out that the same set of constant penalty function values can be used to describe both of the resin systems and all three glass fabrics. The penalty constant for the epoxies (interfacing with copper or glass) was 1; for the glasses (interfacing with epoxy) it was 0.23; and for the copper (interfacing with epoxy) it was 1. These three constants were used throughout the calculations.

The experimental measurements and numerical predictions of the effective CTE values are summarized

Table 2 Effective CTE: Experimental measurements and numerical predictions (in parentheses).

Laminates	Fraction of resin, 1 excluding copper		Below $T_{\rm g}^{er}$		Above $T_{\rm g}^{\rm er}$	
	by wt.	by vol.	in-plane	out-of-plane	in-plane	out-of-plane
FR-4-1675	0.51	0.66	17–18 (17.0)	63–67 (63.5)	6-8 (7.0)	361–386 (350)
FR-4-1080	0.59	0.73	19–20 (20.2)	57–73 (67.5)	5–10 (7.0)	366–395 (386)
FR-4-106	0.64	0.77	20-21 (22.5)	70-75 (69.3)	6-7 (7.0)	399-420 (406)
FR-4-1675 (4 @ 1 oz Cu) <sup>2</sup>	0.50	0.65	16-17 (16.6)	53–54 (59.7)	12-17 (15)	303–312 (312)
FR-4-1080 (4 @ 1 oz Cu) <sup>2</sup>	0.61	0.75	19 (19.0)	69–70 (66)	12-13 (15)	379–390 (384)
FR-4-106 (4 @ 1 oz Cu) <sup>2</sup>	0.70	0.81	20–21 (20.8)	70–78 (68)	12–15 (15)	387–411 (398)
$High-T_g-1080$	0.63	0.74	19–21 (20.1)	59-67 (67.1)	9–10 (9.0)	382–389 (388)
${ m High-}T_{ m g}{ m -}106$	0.66	0.76	20–22 (21.5)	67–79 (67.8)	8-10 (9.0)	399-425 (399)

Weight and volume percentages varied from sample to sample by  $\pm 1\%$ .

**Table 3** Temperature domains used in calculating average CTE values.

Epoxy resin	Below T <sup>er</sup> (°C)	Above $T_{\rm g}^{er}$ (°C)
FR-4	20-100	150-250
High- $T_{\rm g}$	20-100	200-250

in Table 2. Entries for TMA data are given as ranges of values, whereas numerical predictions are given as single numbers in parentheses. Each TMA measurement comprised a continuous determination of effective CTE values for all temperatures from 20 to 260°C. The temperature domains considered to be "below  $T_{\circ}^{er}$ " and "above  $T_g^{er}$ " are given in **Table 3**. For each of the measurements made on a sample, an average CTE value was calculated over each of the two appropriate temperature domains given in Table 3. Each entry in Table 2 for the range of CTE values comprises the minimum and maximum of the corresponding averages, over all the samples. Good agreement is observed between experimental data and numerical predictions: Except for the in-plane CTE above  $T_{\mathfrak{g}}^{er}$ , all discrepancies are within 5%.

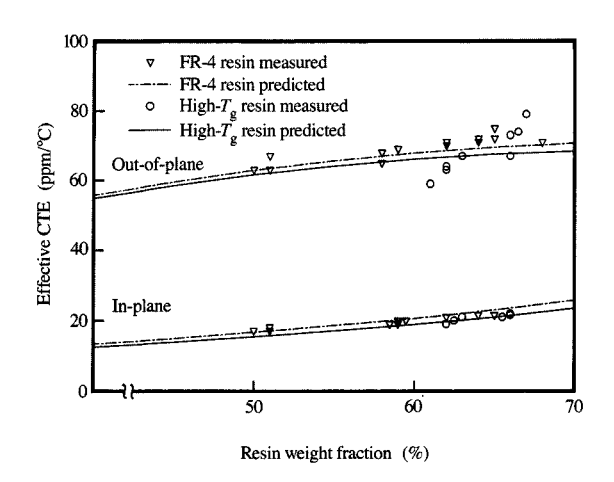
Several conclusions can be drawn. First, the fact that the same set of penalty constants equally described both epoxies indicates that both epoxies interact similarly with the glass fabric and copper. Second, the fact that the same penalty constants equally described three types of glass cloth indicates that all three fabric styles and their

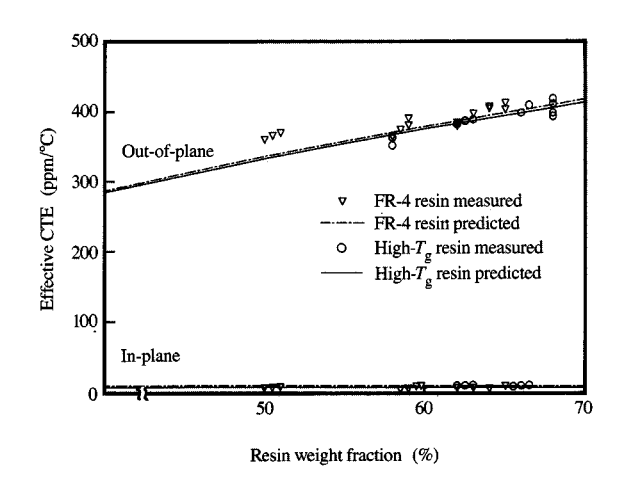
interactions with epoxy are quite similar; furthermore, penalty functions do not depend on the volume fraction (or thickness) of the glass, at least within the range of the laminates tested (volume fraction of the glass between 19% and 35%). Third, a penalty function of 1 for the copper implies that the current copper surface treatment gives good adhesion, which permits one to apply the modulusmodified rule-of-mixtures theory, whereas a penalty function of 0.23 indicates that the properties of wovenglass fabrics are quite different from those of bulk glass, and that the interfacial adhesion coverage might not be complete. It is speculated that the in-plane CTE of epoxy-glass laminate can be further reduced if the glass fabrics are improved (e.g., fewer voids and better surface treatment). Finally, the validity of the engineering model and its associated simplifying assumptions is demonstrated by the excellent correlation between model predictions and measurements in Table 2.

Data in Table 2 are presented in more detail in the following figures. The effective CTEs (in-plane and out-of-plane) of the epoxy-glass laminates versus the resin weight percentage are shown in **Figure 3** and **Figure 4**.

Figure 3 gives the thermal expansion characteristics for temperatures below  $T_{\rm g}^{\rm er}$ . The out-of-plane effective CTE is about three times greater than the in-plane value. The CTE also increases as the percentage of resin increases. The difference in predicted CTE values between the two epoxy systems is only marginal (less than 5%). The high- $T_{\rm g}$  resin shows slightly lower CTE than the FR-4. The TMA data are plotted on the same graph, for comparison.

<sup>&</sup>lt;sup>2</sup>Four layers of 1-oz copper (approximately 36 μm thick) evenly distributed in the epoxy-glass laminate.





# and states

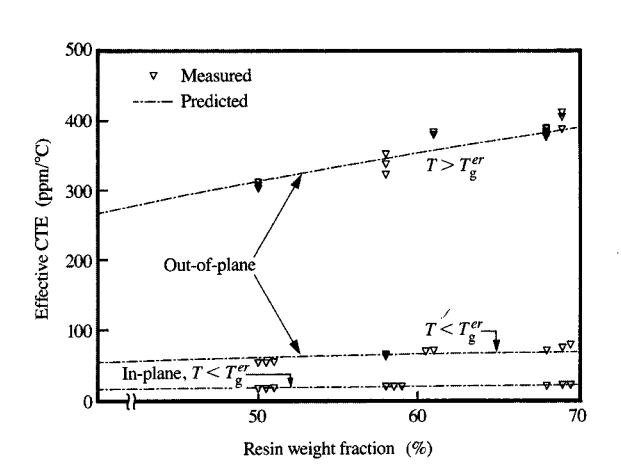
Effect of resin weight percentage on the effective CTE of epoxy-glass laminates, for temperatures below  $T_{g}^{er}$ .

# Floure:

Effect of resin weight percentage on the effective CTE of epoxyglass laminates, for temperatures above  $T_g^{er}$ .

The effect of resin weight percentage on CTE at temperatures above  $T_g^{er}$  is given in Figure 4. Again, both epoxy resins show similar behavior. Note that the out-ofplane effective CTE above  $T_{\rm g}^{\rm er}$  is more than 300 ppm/°C. This is five times higher than the out-of-plane CTE at temperatures below  $T_g^{er}$ . On the other hand, the in-plane CTE above  $T_g^{er}$  does not vary with resin weight percentage and is actually lower than its counterpart below  $T_g^{er}$ . This confirms that above  $T_g^{er}$ , epoxy becomes a soft, viscous fluid, which has little effect on the in-plane CTE of the laminate. However, the incompressible nature of the fluid leads to a much higher expansion of the laminate in the out-of-plane direction, since it is confined by the glass fabric in the in-plane direction. This information is important in assessing the reliability of plated-through holes in a thick PWB when high-temperature processes such as vapor-phase soldering or wave soldering are required, since high CTE in the out-of-plane direction implies more strain in the plated-through holes as a result of temperature excursions.

The effect of copper planes on CTEs for the FR-4 composites (with four layers of 1-oz copper evenly distributed in the composites) is presented in **Figure 5**. The effective CTE is slightly lowered because of the presence of copper, but it follows the same trend as the data presented in Figures 3 and 4. Again, good agreement is observed between the model predictions and TMA measurements.

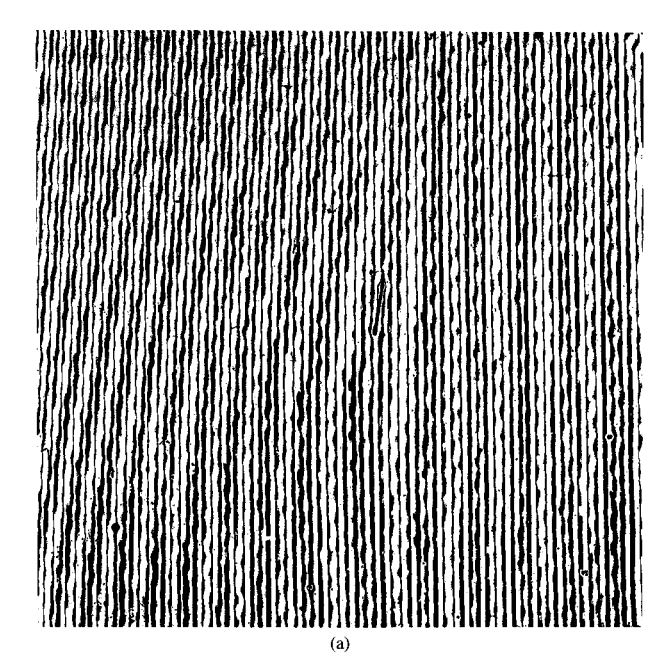


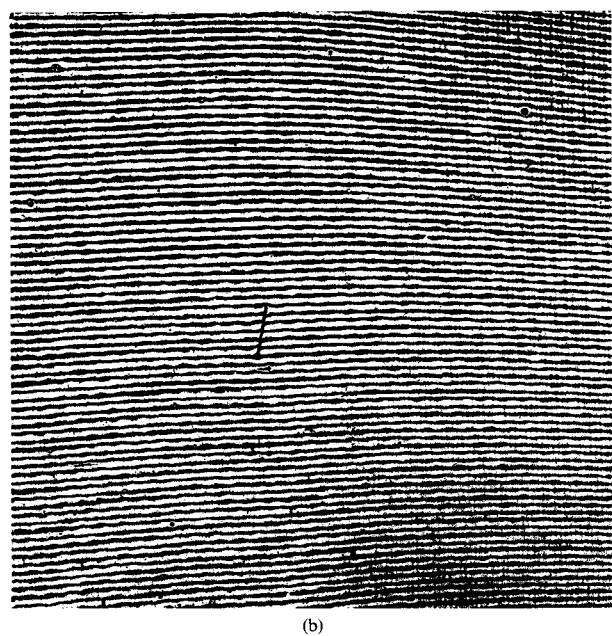
Effect of resin weight percentage on the effective CTE of FR-4 epoxy-glass laminates with four layers of 1-oz copper foils evenly distributed in the laminates.

# Effect of design features: Thermal strain distribution of a multilayer PWB

The previous sections describe the effective CTE of epoxy-glass laminates that have no design features, such

629





# Element Ele

Moiré interferometry fringe patterns of an FR-4 multilayer laminate: (a) x-displacement field,  $CTE(x) = 19.8 \text{ ppm/}^{\circ}C$ . (b) y-displacement field,  $CTE(y) = 19.8 \text{ ppm/}^{\circ}C$ . The fringe frequency is proportional to the thermal expansion of the laminate. The grating size is  $25 \times 25 \text{ mm}$ , and the applied temperature change is  $60^{\circ}C$ .

as plated-through holes and signal lines. Two questions remain unanswered. First, how does this measured CTE compare with the CTE of an actual multilayer PWB? Second, how do the design features affect the CTEs of a typical PWB?

The TMA measures the thermal strain (effective CTE) of a small, specially prepared specimen over a range of temperatures. Real PWBs are highly complex structures and contain a variety of design features such as signal lines, pads and lands on signal and power planes, internal vias, and drilled and plated-through holes. A technique known as moiré interferometry [11] has been adopted to measure the distribution of thermal–mechanical displacements and strains over the entire surface of PWBs, with specific attention to regions with plated-through holes. Knowledge of the thermal–mechanical strain over the plated-through-hole regions is particularly important, since surface mount components are often mounted over such regions.

The principle of moiré interferometry is similar to that of the geometric moiré method [11]. Epoxy gratings  $(20-30~\mu m$  thick) are imprinted on samples at a reference temperature, and measurements are conducted on the grating area before and after load application (heating or cooling). The general procedure of creating specimen gratings and conducting measurements is discussed in [12]. The fringe patterns obtained by moiré interferometry in the experiments described here are contour maps of displacements due to thermal loading (no external mechanical load). The amount of displacement depends on temperature change and the CTE value of the tested material.

In our experiments, specimen gratings of 1200 lines/mm were used, providing a displacement sensitivity of 0.417  $\mu$ m per fringe order. Usually, centers of both dark and bright fringes can be used for displacement calculation; thus, the displacement resolution is 0.208  $\mu$ m. The resolution of the CTE measurement is directly related to the displacement resolution of the experimental technique. The CTE value can be determined as follows:

$$CTE = \frac{\Delta L}{L} \cdot \frac{1}{\Delta T},\tag{14}$$

where  $\Delta L$ , L, and  $\Delta T$  denote the thermal displacement, initial length of the grating area, and temperature change, respectively. With a displacement resolution of 0.208  $\mu$ m, initial grating size of 25 × 25 mm, and  $\Delta T = 60^{\circ}$ C, this translates to an average CTE resolution of  $\pm 0.13$  ppm/°C.

Some experiments were conducted on epoxy-glass composites without any design features, to measure CTE variations in the x and y directions over large areas (5-20 cm<sup>2</sup>). Figure 6 shows fringe patterns of a typical FR-4 multilayer composite after a temperature change of  $60^{\circ}$ C. The initial fringes were canceled by adjusting the interferometer, so that the fringes shown in the figures are directly related to thermal displacement. The fringe patterns are fairly uniform. Average CTEs in the x and y directions show similar values. The wavy shape in the fringes indicates local mismatches of material properties

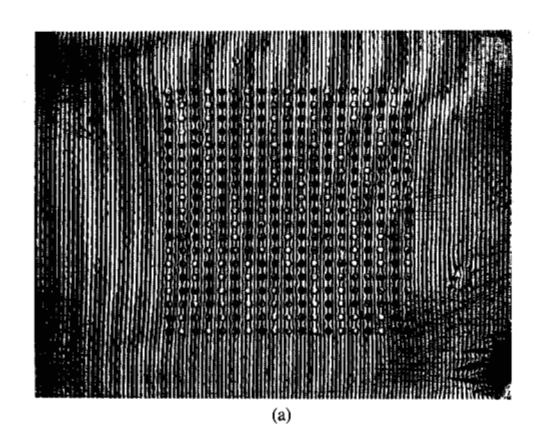
between the glass fabric and the epoxy resin. However, these localized variations do not affect the average CTE value. These fringe patterns are typical for a wide range of composites, with thicknesses varying from 0.25 mm to 8 mm. When cross-plying is used, the difference between the CTE values in the x and y directions is, in general, within 1 ppm/ $^{\circ}$ C.

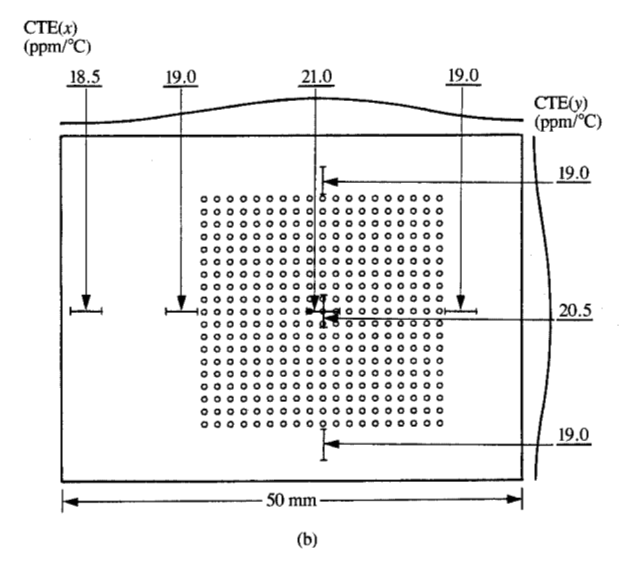
The distribution of the in-plane CTE of a multilayer PWB over areas that have various surface and internal features is shown in Figure 7. It can be seen that the area with plated-through holes has higher CTE values than the rest of the board. Measurements were performed in areas with plated-through holes, with and without solder fill. Results showed a 1.0-1.5-ppm/°C increase of the CTE values in the area with holes over areas without holes. This indicates that the hole-drilling process partially relieves the constraint of the glass fabric and copper foil, which implies that the values of the penalty functions for glass fabric (interfacing with epoxy) are decreased after the hole drilling. This is consistent with cross-sectional observations in which epoxy-glass interfaces showed microcracks after the hole drilling. It is speculated that other hole-drilling processes (with different speed, drill-bit, temperature, etc.) will lead to other sets of penalty functions. However, more investigations are needed in order to quantify this effect. After the plated-through holes were filled with solder, another 1.0-1.5-ppm/°C increase in CTE was observed. This increase is due to the higher CTE of solder, which is around 28 ppm/°C. This 2.0-3.0-ppm/°C increase of the in-plane CTE value after hole drilling and solder fill depends on factors such as process conditions, solder type, plated-through-hole geometry, and copperplating thickness. The value of the increase may vary from PWB to PWB. However, since surface mount components are assembled over different locations on the PWB, the effects of the plated-through holes and solder fill on in-plane CTE should be included in strain modeling associated with component-PWB CTE mismatch.

# Reliability issues related to PWB

• Thermal fatigue life of surface mount interconnection
In the choice of interconnections from modules (first-level packages) to second-level packages, such as PWBs and flexible substrates, one of the prime considerations is the reliability of the interconnection system. The interconnection reliability depends not only upon the interconnection materials and processes, but also upon the properties of the first- and second-level packages being interconnected.

Solder Ball Connect (SBC) [13] (in addition, see other SBC papers in this issue), also known as ball grid array, is a prime example of an area array surface mount assembly in which solder bridges connect the metallized areas of the







In-plane CTE distributions of a multilayer printed wiring board with solder-filled plated-through holes: (a) Fringe pattern in the x direction. (b) CTE values in the x and y directions.

modules and the board. The solder geometry depends on the composition of the solder ball, the solder volume, the solder wetting and flow process, and the geometry of the solder pads on the module and board. Although numerous analyses and reviews have been published regarding fatigue failure of solder interconnections due to thermal cycles [13, 14], much less has been published on the design, material composition, and processes of the first-and second-level packages which govern the mechanical properties that affect the reliability of the interconnection system. The focus of this section is to illustrate the impact of the in-plane CTE of the PWB on the reliability of SBC and other surface mount interconnections.

Typical solder interconnections—for example, the wellknown C-4 (controlled collapse chip connection) [15]—are area arrays of spherical solder balls with round pads on the two ends of the solder joints. Norris and Landzberg [16] reported a quasi-empirical model for C-4 that is based upon the well-known Coffin-Manson [17] relationship between fatigue life and cyclic plastic strain amplitude, with two factors added to account for the temperaturedependent creep and relaxation behavior of solder: a factor to model the increase of fatigue life<sup>2</sup> with frequency, and a factor to model the decrease of fatigue life with maximum temperature. Moreover, Norris and Landzberg assumed that the cyclic strain amplitude is equal to the average shear strain for the joint, computed from the difference in thermal expansion between module and board divided by the solder joint height. The maximum plastic strain amplitude occurs at the solder joint farthest from the geometric center of the array. With this quasi-empirical model, Norris and Landzberg projected the fatigue life for an assembly of System/370<sup>™</sup> logic chips connected to a ceramic module. Their analysis was based upon the assumption that the failure distribution was lognormal and upon a set of laboratory test data obtained under higher temperature and higher frequency than field conditions (normal operating conditions). Their projections were in good agreement with field data. Since 1969, their basic methodology, with modifications to account for solder, microstructure, and deformation mechanics, has been the mainstay of module solder joint reliability models.

The Norris-Landzberg model for the Coffin-Manson relationship demonstrates the inherent capability of solder interconnection materials to absorb high levels of strain and cyclic creep damage. The same capability could serve well for much larger solder interconnections, such as SBC. The Norris-Landzberg model may be stated as follows:

$$N_{\rm f} = \left(\frac{A}{\epsilon_{\rm p}}\right)^{1.9} f^{0.3} e^{-0.123/kT_{\rm max}},\tag{15}$$

where A is a material constant,  $N_{\rm f}$  is the mean fatigue lifetime in cycles, f is the cyclic frequency,  $T_{\rm max}$  is the maximum temperature in degrees Kelvin, k is the Boltzmann constant, and  $\epsilon_{\rm n}$  is the plastic strain amplitude

induced by thermal cycling. The plastic strain amplitude is directly influenced by the lateral movement between module and board, which must be absorbed by the solder. The in-plane modulus and flexural rigidity of the module and board also affect the plastic strain amplitude, as demonstrated by Hall [18].

A significant amount of work has been published on surface mount interconnection fatigue (wear-out) for leadless and leaded assemblies, e.g., [13, 14]. Pertinent to the current study is the result that the mean fatigue life is proportional to the reciprocal of the plastic strain amplitude  $\epsilon_p$  (which is proportional to the difference between the CTE of the module and that of the board) to some power, which has been determined to be approximately 2 for most cases.

To demonstrate the impact of module and board CTE on the fatigue life of SBC interconnections, we consider an assembly consisting of a ceramic module on a PWB as an example. Ceramic modules typically have CTE values around 7 ppm/°C. If the PWB CTE is 17 ppm/°C, simple arithmetic shows that a 1-ppm/°C change in CTE for either the module or the PWB would make a 10% change in the thermal expansion difference and thus in the in-plane strain. The Norris-Landzberg model, as described in Equation (15), would predict a change in fatigue life of approximately 20%. On the other hand, it is noteworthy that in Table 2 and Figures 3-5, the in-plane CTE of the board is actually less at temperatures above  $T_{\rm g}^{\it er}$  than at temperatures below. This implies that a high-temperature cycle, such as for a vapor-phase solder process beyond  $T_{\rm e}^{er}$ , does not necessarily create excessive strain on the solder joints. Also, in Figure 7, one can observe that the in-plane CTE in areas with plated-through holes (filled with solder) is 21 ppm/°C, while the rest of the PWB is about 19 ppm/°C. In estimating the fatigue life of solder balls that are connected to areas with plated-through holes, using a 19-ppm/°C CTE value for the board leads to an overestimate of the fatigue life. To accurately assess the solder damage during thermal shock (sudden temperature change), it is important to have a thorough quantitative understanding of the design factors that affect the thermal expansion characteristics and stiffness of the PWB.

• Thermal shock strain for plated-through holes
Plated-through holes in PWBs have been observed to
crack during the soldering process. Stress tests have been
developed to simulate thermal shock behavior. In
particular, MIL-STD-202D M107C has been used for
reliability testing of plated-through holes for military
products. The plated-through-hole reliability in PWBs has
been well studied from the perspective of copper-plating
ductility, hole-surface preparation processes, stress-test
methods, and mechanical modeling [1-3]. The tensile

 $<sup>\</sup>overline{^2}$  Here, fatigue life refers to the number of cycles to failure. The total temporal lifetime of solder interconnections actually decreases with frequency. In the electronics industry, however, fatigue life is often given as the number of cycles to failure, since it relates directly to the number of on and off cycles a machine or device can withstand.

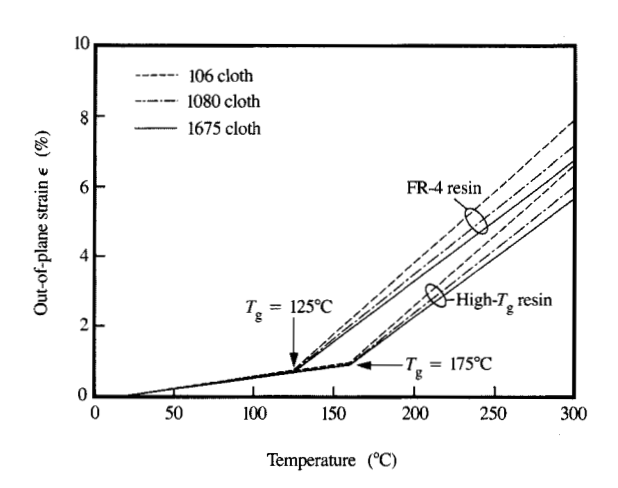
ductility of copper plating and that of the copper foil internal to boards vary according to manufacturing processes, geometry, and temperature [19–21]. Typically, the ductility can vary from 4 to 12% [19]. How the PWB construction itself can influence the plated-through-hole reliability had been little discussed.

An important conclusion from the present study is that the out-of-plane thermal strain of a multilayer PWB is primarily due to strain above the glass transition temperature,  $T_g^{er}$ . The physical explanation of this observation is that the epoxy material, behaving like an incompressible fluid, is primarily constrained in the x-yplane by the glass fabric and copper, and almost all of the volume expansion is in the z direction. The thermal strain is therefore significantly influenced by the percentage of resin and glass fabric and by  $T_a^{er}$ . The engineering model, as presented in Equations (3)-(13), can provide useful insights into the out-of-plane thermal strain for PWBs with various resins and glass fabrics. Figure 8 shows the relation between thermal strain and temperature for the FR-4 and high- $T_g$  resins, with three different glass fabrics. The out-of-plane CTEs, below and above  $T_{g}^{er}$ , are both assumed to be constant. It is seen that for the FR-4, the thermal strain at 300°C increases from 6.7% to 7.9% from the nominal laminate (type 1675 glass, 51% resin by weight) to the resin-rich laminate (type 106, 64% resin by weight). On the other hand, the 50°C increase in  $T_{o}^{er}$  due to the difference in resins leads to a 1.5% strain decrease for type 1675 and a 1.8% strain decrease for type 106, at 300°C.

The out-of-plane expansion of the multilayer laminate has direct impact on the plated-through-hole strain. Copper plating in the holes is subjected to tensile or compressive deformation during the out-of-plane expansion or shrinkage of the surrounding epoxy. The degree of deformation depends on factors such as plated-through-hole stiffness, copper-to-resin adhesion, copper power plane thickness, and connections between copper power plane and plated-through holes. This physical phenomenon of in-plane constraint and out-of-plane expansion is particularly important to non-solder-filled plated-through-hole design and the design of internal via connections in multilayer laminate structures with high-CTE and low- $T_g^{er}$  (or melting-point) epoxies (or other dielectric materials).

# Summary

A systematic study of the thermal-mechanical strains in a multilayer printed wiring board has led to a quantitative three-dimensional engineering model based upon classical mechanics and modified rule-of-mixtures theory. This model was verified by a series of experimental measurements. With this model, the in-plane and out-of-plane thermal strains can be accurately predicted from a knowledge of the proportions of resin and glass in the



Predicted out-of-plane thermal strain for laminates made of FR-4 and of high- $T_{\rm g}$  resin, using various glass fabrics.

epoxy-glass laminate and the copper construction. The model provides an engineering tool that can be used to assess reliability concerns associated with the printed wiring board, such as fatigue life of solder interconnections and plated-through holes, in the early design stage.

# **Acknowledgments**

The authors thank T. Houston and J. Gotro for technical guidance and J. Roth, B. Whalen, and A. Seman for providing epoxy-glass laminates. The TMA CTE measurements from E. Livingston and tensile test results of epoxies from D. Questad were also greatly appreciated.

System/370 is a trademark of International Business Machines Corporation.

# References

- K. Ramakrishna, G. Subbarayan, and B. G. Sammakia, "Effect of Non-Uniformities and Defects on PTH Strain During Assembly and Accelerated Thermal Cycling," Advances in Electronic Packaging, W. T. Chen and H. Abe, Eds., Proceedings of the 1992 Joint ASME/JSME Conference on Electronic Packaging, Milpitas, CA, April 9-12, 1992, ASME Electrical and Electronic Packaging, Vol. 2, pp. 891-908.
- B. Ozmat, H. Walker, and M. Elkins, "A Nonlinear Thermal Stress Analysis of the Plated Through Holes of Printed Wiring Boards," Proceedings of the International Electronics Packaging Technical Conference 1990, Marlborough, MA, 1990, pp. 359-381.
- D. Barker, M. Pecht, A. Dasgupta, and S. Naqvi, "Transient Thermal Stress Analysis of a Plated Through Hole Subjected to Wave Soldering," *Trans. ASME*, J. Electron. Packaging 114, No. 2, 149-155 (1991).

- D. P. Seraphim, D. E. Barr, W. T. Chen, G. P. Schmitt, and R. R. Tummala, in *Microelectronics Packaging Handbook*, R. R. Tummala and E. P. Rymaszewski, Eds., Van Nostrand Reinhold, New York, 1989, Section 12.4, Ch. 12.
- A. M. Ibrahim, "Quartz-Fabric-Reinforced Thermoset and Thermoplastic Composites as SMT-PCBS for Military Applications," Proceedings of the 3rd International SAMPE Electronics Conference, Society for the Advancement of Material and Process Engineering, 1989, pp. 1266-1280.
- L. R. Wallig, "Approaching the Ideal Laminate for Surface Mount IC Packaging," Proceedings of the 2nd International SAMPE Electronics Conference, Society for the Advancement of Material and Process Engineering, 1988, pp. 300-308.
- J. C. Chamblin, "Cyanate Ester Offers Light Weight, Low Cost, Low CTE PWBs for Advanced Surface Mount Technology Applications," Proceedings of the International Electronics Packaging Technical Conference 1991, San Diego, 1991, pp. 677-684.
   F. L. Gray, "Thermal Expansion Properties," Electronic
- F. L. Gray, "Thermal Expansion Properties," Electronic Materials Handbook, Vol. 1—Packaging, ASM International, Materials Park, OH, 1989, pp. 611-629.
- 9. R. Hill, "Theory of Mechanical Properties of Fibre-Strengthened Materials: 1. Elastic Behavior," *J. Mech. Phys. Solids* 12, 199-212 (1964).
- R. A. Schapery, "Thermal Expansion Coefficients of Composite Materials Based on Energy Principles," J. Compos. Mater. 2, No. 3, 380-404 (1968).
- D. Post, "Moiré Interferometry," Handbook of Experimental Mechanics, A. S. Kobayashi, Ed., Prentice-Hall, Inc., Englewood Cliffs, NJ, 1987, Ch. 7.
- 12. Y. Guo, C. K. Lim, W. T. Chen, and C. G. Woychik, "Solder Ball Connect (SBC) Assemblies Under Thermal Loading: I. Deformation Measurement via Moiré Interferometry, and Its Interpretation," *IBM J. Res. Develop.* 37, 635-647 (1993, this issue).
- Solder Joint Reliability: Theory and Application, J. H. Lau, Ed., Van Nostrand Reinhold, New York, 1990.
- 14. J. P. Clech, W. Engelmaier, R. W. Kotlowitz, and J. A. Augis, "Reliability Figures-of-Merit for Surface Soldered Leadless Chip Carriers Compared to Leaded Packages," *IEEE Trans. Components, Hybrids, Manuf. Technol.* 12, No. 4, 449–458 (1989).
- N. G. Koopman, T. C. Reiley, and P. A. Totta, in Microelectronics Packaging Handbook, R. R. Tummala and E. P. Rymaszewski, Eds., Van Nostrand Reinhold, New York, 1989, Ch. 6.
- K. C. Norris and A. H. Landzberg, "Reliability of Controlled Collapse Interconnections," *IBM J. Res. Develop.* 13, 266–271 (1969).
- 17. S. S. Manson, "Thermal Stress and Low Cycle Fatigue, McGraw-Hill Book Co., Inc., New York, 1966.
- P. M. Hall, "Force Moments and Displacements During Thermal Chamber Cycling of Leadless Ceramic Chip Carriers Soldered to Printed Boards," *IEEE Trans.* Components, Hybrids, Manuf. Technol. CHMT-7, No. 4, 314–327 (1984).
- K. Lin and R. Weil, "Mechanical Properties of Electroless Copper Under Conditions Prevailing During Soldering of Printed Circuit Boards," *Plating & Surf. Finish.* 77, No. 2, 44-47 (1990).
- 20. R. N. Wild, "Internal Electrodeposited Copper Foil Cracking in Multilayer Boards," *Technical Paper IPC-TP-286*, IPC Fall Meeting, Institute for Interconnecting and Packaging Electronic Circuits, San Francisco, September 1979, pp. 9–18.
- 21. T. Y. Wu and C. G. Woychik, "Void Assisted Cracking in Copper Foil at High Temperatures," Proceedings of ASME Winter Annual Meeting in Manufacturing

Processes and Materials—Challenges in Microelectronic Packaging, W. T. Chen, P. Engel, and W. E. Jahsman, Eds., Atlanta, 1991, Applied Mechanics Division, Vol. 131, pp. 11–15.

Received February 5, 1993; accepted for publication May 13, 1993

Tien Y. Wu IBM Microelectronics Division, 1701 North Street, Endicott, New York 13760 (WUTIEN at ENDVMTKL, wutien@endvmtkl). Dr. Wu received his M.S. and Ph.D. degrees in mechanical engineering and applied mechanics from the University of Pennsylvania in 1984 and 1988, respectively. He remained there as a Postdoctoral Fellow for another year, joining IBM in 1989. His research and development activities have been in the areas of material and composite characterization, mechanical design, process optimization, analytical and experimental analysis of interfacial crack propagation, and reliability prediction for electronic packages. In 1992, Dr. Wu received an IBM Outstanding Technical Achievement Award for excellence in process mechanics.

Yifan Guo IBM Microelectronics Division, 1701 North Street, Endicott, New York 13760 (YIFAN at ENDVMTKL, yifan@endvmtkl.vnet.ibm.com). Dr. Guo received his Ph.D. degree in engineering mechanics from Virginia Polytechnic Institute and State University in 1989. After graduation, he was appointed as Assistant Professor in the Engineering Science and Mechanics Department at VPI&SU. He taught courses in mechanics and continued his research in the area of experimental mechanics and mechanics of composite materials. Dr. Guo joined IBM in 1990 as a staff engineer and began his research in the field of microelectronic packaging, using laser interferometry and other experimental techniques. He recently received an IBM Division Award for his contributions in the development and applications of moiré interferometry in electronic packaging.

William T. Chen IBM Microelectronics Division, 1701
North Street, Endicott, New York 13760 (CHENWT at
ENDVMTKL, chenwt@endvmtkl). Dr. Chen received a B.S.
degree in mechanical engineering from Queen Mary College,
London University; an M.S. from Brown University; and a
Ph.D. from Cornell University in theoretical and applied
mechanics. He joined IBM in 1963. Dr. Chen has been
active in various aspects of electronic packaging product
development and manufacturing, including design, materials,
processes, and reliability. His interest has been in applying
knowledge of mechanics, materials, and physics to engineering
practices of design and manufacturing for leading-edge
electronic packaging products. Dr. Chen is a Fellow of the
American Society of Mechanical Engineers; he has been
elected to the IBM Academy of Technology.